

Effects of Zn and Ni substitution on the Cu spin dynamics and superconductivity in $\text{La}_{2-x}\text{Sr}_x\text{Cu}_{1-y}(\text{Zn},\text{Ni})_y\text{O}_4$ ($x=0.15-0.20$): Muon spin relaxation and magnetic susceptibility study

T. Adachi,* N. Oki, Risdiana,† S. Yairi, and Y. Koike

Department of Applied Physics, Graduate School of Engineering, Tohoku University,
6-6-05 Aoba, Aramaki, Aoba-ku, Sendai 980-8579, Japan

I. Watanabe

Advanced Meson Science Laboratory, RIKEN Nishina Center, 2-1 Hirosawa, Wako 351-0198, Japan
(Received 6 December 2007; revised manuscript received 5 August 2008; published 14 October 2008)

We have investigated effects of Zn and Ni on the Cu spin dynamics and superconductivity from the zero-field muon spin relaxation (ZF- μ SR) and magnetic susceptibility χ measurements for $\text{La}_{2-x}\text{Sr}_x\text{Cu}_{1-y}(\text{Zn},\text{Ni})_y\text{O}_4$ with $x=0.15-0.20$, changing y up to 0.10 in fine step. In the optimally doped $x=0.15$, it has been concluded that the formation of a magnetic order requires a larger amount of Ni than of Zn, which is similar to our previous results of $x=0.13$. From the estimation of volume fractions of superconducting (SC) and magnetic regions, it has been found for $x=0.15$ that the SC region is in rough correspondence to the region where Cu spins fluctuate fast beyond the μ SR frequency window for both Zn- and Ni-substituted samples. According to the stripe model, it follows that, even for $x=0.15$, the dynamical stripe correlations of spins and holes are pinned and localized around Zn and Ni, leading to the formation of the static stripe order and the suppression of superconductivity. These may indicate an importance of the dynamical stripe in the appearance of the high- T_c superconductivity in the hole-doped cuprates. In the overdoped regime of $x=0.18$ and 0.20, on the other hand, the SC region seems to be in rough correspondence to the region where Cu spins fluctuate fast beyond the μ SR frequency window, although it appears that the Cu spin dynamics and superconductivity are affected by the phase separation into SC and normal-state regions.

DOI: [10.1103/PhysRevB.78.134515](https://doi.org/10.1103/PhysRevB.78.134515)

PACS number(s): 76.75.+i, 74.25.Ha, 74.62.Dh, 74.72.Dn

I. INTRODUCTION

Toward understanding of the mechanism of high- T_c superconductivity, an approach through the substitution of impurities for Cu has been one of major ways to study the Cu spin dynamics in the high- T_c physics. In the hole-doped high- T_c cuprates, it is well known that nonmagnetic impurities such as Zn tend to suppress the superconductivity more markedly than magnetic impurities such as Ni,¹ which is an opposite trend to the conventional superconductors.² Early NMR and nuclear quadrupole resonance (NQR) measurements have revealed that Zn acts as a strong scatterer of holes causing the unitarity scattering, while Ni acts as a weak scatterer causing the Born scattering.³ From inelastic neutron-scattering experiments focusing on the high-energy Cu spin fluctuations, it has been reported that the so-called resonance energy does not change through the Zn substitution, while it decreases through the Ni substitution.⁴ As for the low-energy Cu spin fluctuations, on the other hand, Kimura *et al.*⁵ and Kofu *et al.*⁶ have insisted from the inelastic neutron-scattering measurements in $\text{La}_{2-x}\text{Sr}_x\text{Cu}_{1-y}(\text{Zn},\text{Ni})_y\text{O}_4$ with $x=0.15$ that Zn tends to bring about the so-called in-gap state in the spin gap, while Ni tends to reduce the spin gap itself. These results are strongly suggestive of different effects between the Zn and Ni substitution on the Cu spin dynamics and superconductivity, but the reason has not yet been clarified.

Formerly, we have performed zero-field (ZF) muon spin relaxation (μ SR) and magnetic susceptibility χ measurements in $\text{La}_{2-x}\text{Sr}_x\text{Cu}_{1-y}(\text{Zn},\text{Ni})_y\text{O}_4$ around $x=0.115$ at low temperatures down to 2 K, changing y up to 0.10 in fine step,⁷⁻¹² in order to investigate impurity effects on the so-

called spin-charge stripe order¹³ which may be related to the mechanism of high- T_c superconductivity.¹⁴ For the Zn substitution, a muon spin precession corresponding to the formation of a long-range magnetic order has been observed for $y(\text{Zn})=0.0075-0.03$ in $x=0.10, 0.115, 0.13$.¹¹ Moreover, the further Zn substitution of $y(\text{Zn})>0.03$ brings about a change to slow depolarization of muon spins so that Gaussian-type depolarization has been observed for $y(\text{Zn})=0.10$. These results indicate that a magnetic order is stabilized by a slight amount of Zn, while it is destroyed by a large amount of Zn, which is understandable in terms of the pinning and destruction of the stripe order by Zn.¹⁵⁻¹⁷ For the Ni substitution, on the other hand, a muon spin precession has been observed for $y(\text{Ni})=0.02-0.10$ in $x=0.13$.¹² This indicates that the formation of a magnetic order requires a larger amount of Ni than of Zn and that the magnetic order survives or, rather, it is stabilized by a large amount of Ni. From the χ measurements on field cooling, it has been found that the Meissner volume fraction corresponding to the superconducting (SC) volume fraction rapidly decreases with a slight substitution of Zn and its decrease is more marked by Zn than by Ni. In comparison between the volume fraction of the SC state estimated from χ and that of the magnetic state from μ SR, it has been found that the SC region in a sample is in good correspondence to the region in which Cu spins fluctuate fast beyond the μ SR frequency window (10^6-10^{11} Hz). From the viewpoint of impurity effects on the stripe order, these results suggest that: (i) the dynamical stripe correlations tend to be pinned and stabilized by both Zn and Ni so that the superconductivity is destroyed around themselves and that (ii) Zn is more effective for the pinning of stripes so that the static stripe-ordered

region around Zn is larger than around Ni. These may be the reason why Zn destroys the superconductivity in the hole-doped high- T_c cuprates more markedly than Ni.¹

In this paper, in order to investigate the relationship between the Cu spin dynamics and superconductivity in the optimally doped high- T_c cuprates, we have performed ZF- μ SR and χ measurements in the Zn- or Ni-substituted $\text{La}_{2-x}\text{Sr}_x\text{Cu}_{1-y}(\text{Zn},\text{Ni})_y\text{O}_4$ with $x=0.15$, changing y up to 0.10 in fine step.^{18,19} Moreover, we have extended the measurements for the Zn-substituted $\text{La}_{2-x}\text{Sr}_x\text{Cu}_{1-y}\text{Zn}_y\text{O}_4$ up to $x=0.20$, focusing on the relationship between the Cu spin dynamics and superconductivity in the overdoped regime.

II. EXPERIMENT

Polycrystalline samples of $\text{La}_{2-x}\text{Sr}_x\text{Cu}_{1-y}(\text{Zn},\text{Ni})_y\text{O}_4$ with $x=0.15-0.20$ and $y=0-0.10$ were prepared by the ordinary solid-state reaction method. Details of the procedure have been reported in our former paper.¹¹ For the Ni-substituted samples, however, the sintering was done in air at 1150 °C for 24 h to keep the homogeneity of constituents in a sample.

The ZF- μ SR measurements were performed at the RIKEN-RAL Muon Facility at the Rutherford-Appleton Laboratory in the U.K. using a pulsed positive surface muon beam with an incident muon momentum of 27 MeV/c. The asymmetry parameter $A(t)$ at a time t was given by $A(t) = \{F(t) - \alpha B(t)\} / \{F(t) + \alpha B(t)\}$, where $F(t)$ and $B(t)$ are total muon events of the forward and backward counters, which were aligned in the beam line, respectively. α is the calibration factor reflecting the relative counting efficiencies between the forward and backward counters. The μ SR time spectrum, namely, the time evolution of $A(t)$ was measured at low temperatures down to 0.3 K to detect the appearance of a magnetic order.

The χ measurements were carried out down to 2 K using a superconducting quantum interference device magnetometer (Quantum Design, Model MPMS-XL5) in a magnetic field of 10 Oe on field cooling in order to evaluate the volume fraction of the SC region in a sample.

III. RESULTS

A. Effects of Zn and Ni substitution in $x=0.15$

1. ZF- μ SR

Figure 1 shows the ZF- μ SR time spectra in $\text{La}_{2-x}\text{Sr}_x\text{Cu}_{1-y}(\text{Zn},\text{Ni})_y\text{O}_4$ with $x=0.15$. In order to see the y dependence of the spectra at the lowest temperature of 0.3 K clearly, the time spectra at 0.3 K are also shown in Fig. 2. All the spectra in Figs. 1 and 2 are shown after subtracting the background from the raw spectra and being normalized by the value of the asymmetry at $t=0$. At high temperatures above 15 K, all the spectra show Gaussian-type slow depolarization of muon spins due to the nuclear-dipole field that is randomly distributed at the muon site. This indicates no effect of Cu spins on the μ SR time spectrum. Focusing on the spectra below 2 K, Gaussian-type depolarization is still observed down to 0.3 K for $y=0$, indicating that Cu spins fluctuate fast beyond the μ SR frequency window. For the Zn

substitution, the muon spin depolarization becomes fast with increasing $y(\text{Zn})$ for $y(\text{Zn}) \geq 0.0075$. Moreover, an almost flat spectrum with the normalized asymmetry of $\sim 1/3$ is observed above 0.4 μs for $y(\text{Zn})=0.02$ and 0.03, indicating the formation of a static magnetic state. It is noted that the absence of a muon spin precession may be due to a short-range magnetic order, resulting in very fast damping of the precession, in contrast to the results around $x=0.115$.⁷⁻¹² For $y(\text{Zn}) > 0.03$, the muon spin depolarization becomes slow and a Gaussian-type spectrum is observed, although the muon spin depolarization is still fast at 0.3 K for $y(\text{Zn})=0.10$. This indicates that the magnetic order is destroyed by a large amount of Zn, which is analogous to the results around $x=0.115$.⁷⁻¹² For the Ni substitution, on the other hand, fast depolarization is observed for $y(\text{Ni}) \geq 0.0075$. Eventually, a muon spin precession is observed for $y(\text{Ni})=0.10$, indicating the formation of a long-range magnetic order of Cu spins.

As for the comparison of the spectra between the Zn and Ni substitution, the fast depolarization of muon spins starts to be observed at $y=0.0075$ both in the Zn- and Ni-substituted samples. As shown in Fig. 2, however, the muon spin depolarization at 0.3 K is faster in the 0.75% Zn-substituted sample than in the 0.75% Ni-substituted one. These results indicate that the formation of the magnetic order requires a larger amount of Ni than of Zn, which is similar to our previous results of $x=0.13$.¹² In the heavily impurity-substituted samples, Zn tends to destroy the Cu spin correlation, while Ni tends to stabilize the magnetic order, which is also similar to our previous results of $x=0.13$.¹²

In order to obtain detailed information on the Cu spin dynamics, we analyzed the time spectra shown in Figs. 1 and 2 using the following three-component function:

$$A(t) = A_0 e^{-\lambda_0 t} G_Z(\Delta, t) + A_1 e^{-\lambda_1 t} + A_2 e^{-\lambda_2 t} \cos(\omega t + \phi). \quad (3.1)$$

The first term represents the slowly depolarizing component in a region where the Cu spins fluctuate fast beyond the μ SR frequency window. A_0 and λ_0 are the initial asymmetry and depolarization rate of the slowly depolarizing component, respectively. $G_Z(\Delta, t)$ is the static Kubo-Toyabe function with a half width Δ describing the distribution of the nuclear-dipole field at the muon site.²⁰ The second term represents the fast depolarizing component in a region where the Cu spin fluctuations slow down and/or where a short-range magnetic order of Cu spins is formed. A_1 and λ_1 are the initial asymmetry and depolarization rate of the fast depolarizing component, respectively. The third term represents the muon spin precession in a region where a long-range magnetic order of Cu spins is formed. A_2 is the initial asymmetry. λ_2 , ω , and ϕ are the damping rate, frequency, and phase of the muon spin precession, respectively. Values of A_0 , A_1 , and A_2 obtained from the analysis using Eq. (3.1) are regarded as corresponding to volume fractions of each region depending on the frequency of the Cu spin fluctuations.

As for $y(\text{Zn})=0.10$, the spectra below 1 K cannot be well represented using Eq. (3.1) because of the rather fast Gaussian-type depolarization compared to that due to the

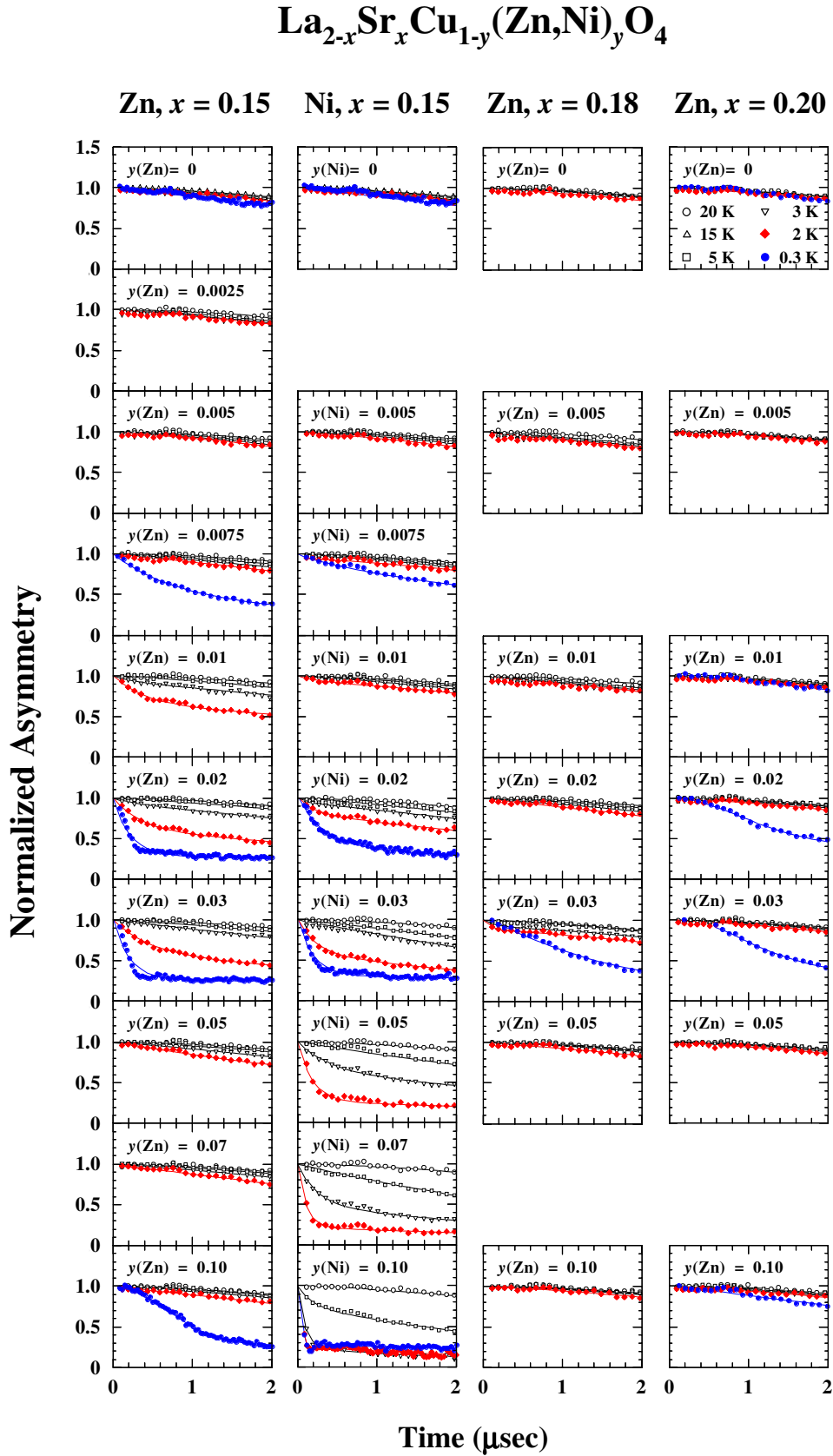


FIG. 1. (Color online) Zero-field μSR time spectra in the early time region from 0 to 2 μs of $\text{La}_{2-x}\text{Sr}_x\text{Cu}_{1-y}(\text{Zn},\text{Ni})_y\text{O}_4$ with $x=0.15$, 0.18, and 0.20 at various temperatures down to 0.3 K. Solid lines indicate the best-fit results using $A(t)=A_0e^{-\lambda_0 t}G_Z(\Delta,t)+A_1e^{-\lambda_1 t}+A_2e^{-\lambda_2 t}\cos(\omega t+\phi)$ except for $y(\text{Zn})=0.10$ in $x=0.15$. For $y(\text{Zn})=0.10$ in $x=0.15$, the following equation is used: $A(t)=A_0e^{-\lambda_0 t}G_Z(\Delta,t)+A_\sigma e^{-(\sigma t)^2}$.

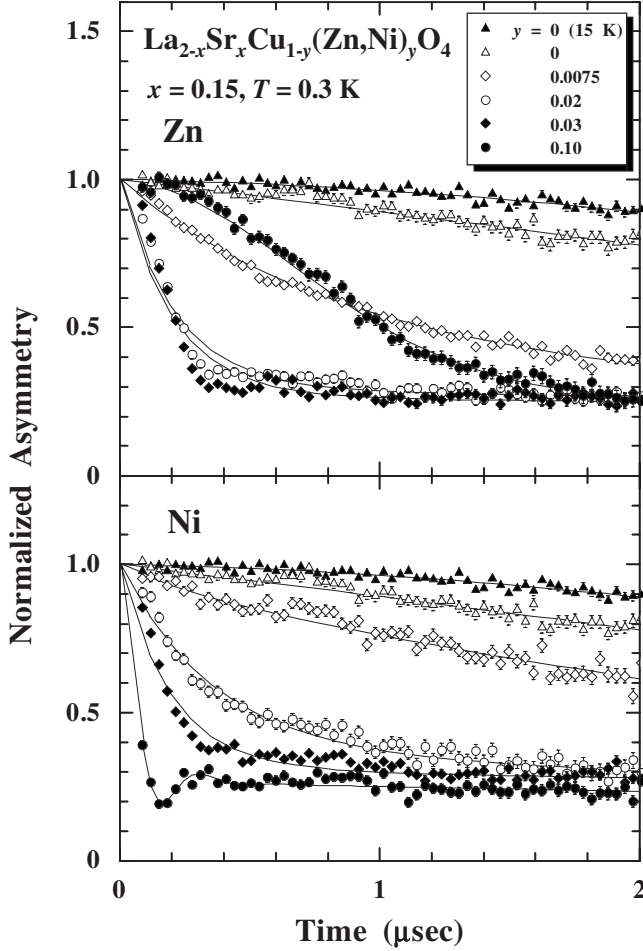


FIG. 2. Zero-field μ SR time spectra at 0.3 K for typical y values of $\text{La}_{2-x}\text{Sr}_x\text{Cu}_{1-y}(\text{Zn},\text{Ni})_y\text{O}_4$ with $x=0.15$. The time spectrum at 15 K for $y=0$ is also plotted. Solid lines indicate the best-fit results using $A(t)=A_0e^{-\lambda_0 t}G_Z(\Delta,t)+A_1e^{-\lambda_1 t}+A_2e^{-\lambda_2 t}\cos(\omega t+\phi)$ except for $y(\text{Zn})=0.10$. For $y(\text{Zn})=0.10$, the equation $A(t)=A_0e^{-\lambda_0 t}G_Z(\Delta,t)+A_\sigma e^{-(\sigma t)^2}$ is used.

nuclear-dipole field. Therefore, the following function was used:

$$A(t) = A_0 e^{-\lambda_0 t} G_Z(\Delta, t) + A_\sigma e^{-(\sigma t)^2}. \quad (3.2)$$

The first term is the same as that in Eq. (3.1). The second term is a simple Gaussian representing a region with larger magnetic moments than nuclear moments being randomly distributed.²¹ The time spectra are well fitted with Eqs. (3.1) and (3.2) as shown by solid lines in Figs. 1 and 2.

Figure 3 shows the temperature dependence of A_0 normalized by its value at a high temperature of 15 or 20 K for $\text{La}_{2-x}\text{Sr}_x\text{Cu}_{1-y}(\text{Zn},\text{Ni})_y\text{O}_4$ with $x=0.15$. The temperature dependence of A_0 is often used as a probe of the magnetic transition because it reflects the volume fraction of the non-magnetic region.^{22–24} In fact, $A_0=1$ means that the spectrum is represented only with the first term of Eq. (3.1) or Eq. (3.2), indicating that all the Cu spins fluctuate fast beyond the μ SR frequency window. On the contrary, $A_0 \sim 1/3$ indicates that all the Cu spins are in a short- or long-range static magnetically ordered state. In Fig. 3, the shaded area at low

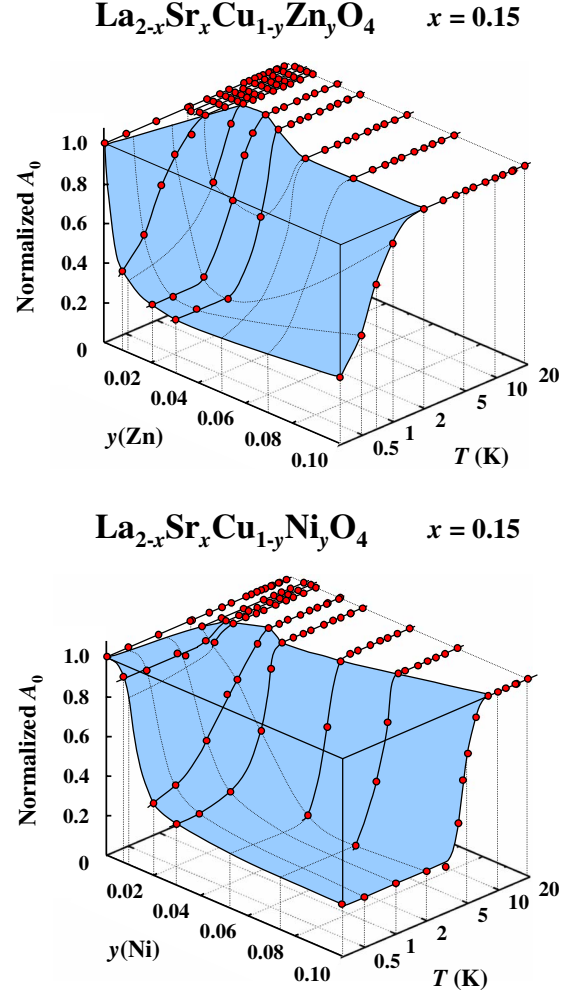


FIG. 3. (Color online) Temperature dependence of the initial asymmetry of the slowly depolarizing component A_0 normalized by its value at a high temperature of 15 or 20 K for $\text{La}_{2-x}\text{Sr}_x\text{Cu}_{1-y}(\text{Zn},\text{Ni})_y\text{O}_4$ with $x=0.15$. The shaded area at low temperatures corresponds to the state in which the Cu spin fluctuations slow down and/or a magnetic order is formed. Solid and dotted lines are to guide the reader's eye.

temperatures corresponds to the state in which the Cu spin fluctuations slow down and/or a magnetic order is formed. For the Zn substitution, A_0 decreases around $y(\text{Zn})=0.01-0.03$ at 2 K, while the area in which A_0 decreases expands at low temperatures below 2 K, indicating that the Cu spin correlation is developed with decreasing temperature in the Zn-substituted samples. Focusing on the temperature T_N^{onset} , at which A_0 starts to decrease with decreasing temperature, it increases with increasing $y(\text{Zn})$ and shows the maximum around $y(\text{Zn})=0.01-0.02$ and decreases above $y(\text{Zn})=0.02$, suggesting that the Cu spin correlation develops most around $y(\text{Zn})=0.01-0.02$. In fact, A_0 is almost $1/3$ below ~ 1 K for $y(\text{Zn})=0.02$ and 0.03 , indicating a static magnetic state. For $y(\text{Zn}) > 0.03$, the area in which A_0 decreases shrinks with increasing $y(\text{Zn})$, but A_0 is below unity at low temperatures due to the random magnetism with magnetic moments slightly larger than nuclear moments even for $y(\text{Zn})=0.10$.

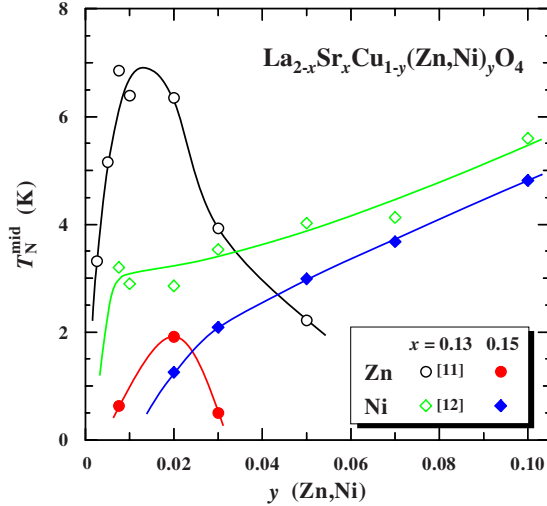


FIG. 4. (Color online) Impurity-concentration dependence of T_N^{mid} defined as the midpoint of the change in the A_0 value from unity to the averaged value of A_0 in the ordered state at 2 K for $\text{La}_{2-x}\text{Sr}_x\text{Cu}_{1-y}(\text{Zn}, \text{Ni})_y\text{O}_4$ with $x=0.15$. The data of $x=0.13$ are also plotted for comparison (Refs. 11 and 12). Solid lines are to guide the reader's eye.

For the Ni substitution, on the other hand, the decrease in A_0 becomes marked with increasing $y(\text{Ni})$ at 2 K and the area in which A_0 decreases expands at low temperatures below 2 K. This indicates that the Cu spin correlation is developed at low temperatures also in the Ni-substituted samples. As for T_N^{onset} , it increases with increasing $y(\text{Ni})$ and shows a local maximum around $y(\text{Ni})=0.02$ and changes to decrease above $y(\text{Ni})=0.02$, which is similar to the Zn-substituted case. For $y(\text{Ni}) > 0.03$, however, T_N^{onset} increases progressively with increasing $y(\text{Ni})$. In fact, A_0 at low temperatures below 2 K is about 1/3 for $y(\text{Ni}) \geq 0.07$, indicating the formation of a static magnetic state.

It is found in the lightly substituted samples of $y \leq 0.03$ that the decrease in A_0 with decreasing temperature is smaller in the Ni substitution than in the Zn substitution, suggesting that Zn is more effective for the development of the magnetic order than Ni. In the heavily substituted samples of $y > 0.03$, the Cu spin correlation tends to be destroyed by Zn while it tends to be developed by Ni.

Figure 4 shows the impurity-concentration dependence of the magnetic transition temperature T_N^{mid} defined as the midpoint of the change in the A_0 value from unity to the averaged value of A_0 in the static magnetic state at 2 K (Ref. 11) in $\text{La}_{2-x}\text{Sr}_x\text{Cu}_{1-y}(\text{Zn}, \text{Ni})_y\text{O}_4$ with $x=0.15$. The data of $x=0.13$ are also plotted for comparison.^{11,12} In the Zn-substituted samples with $x=0.15$, T_N^{mid} appears at $y(\text{Zn})=0.0075$ and shows the maximum at $y(\text{Zn})=0.02$ followed by the disappearance for $y(\text{Zn}) > 0.03$. In the Ni-substituted samples with $x=0.15$, on the other hand, T_N^{mid} appears at $y(\text{Ni})=0.02$ and increases monotonically with increasing $y(\text{Ni})$. The y dependence of T_N^{mid} in $x=0.15$ is qualitatively similar to that in $x=0.13$ in both cases of Zn and Ni substitution.

2. Magnetic susceptibility

Figure 5 shows the temperature dependence of χ on field cooling for $\text{La}_{2-x}\text{Sr}_x\text{Cu}_{1-y}(\text{Zn}, \text{Ni})_y\text{O}_4$ with $x=0.15$ and y

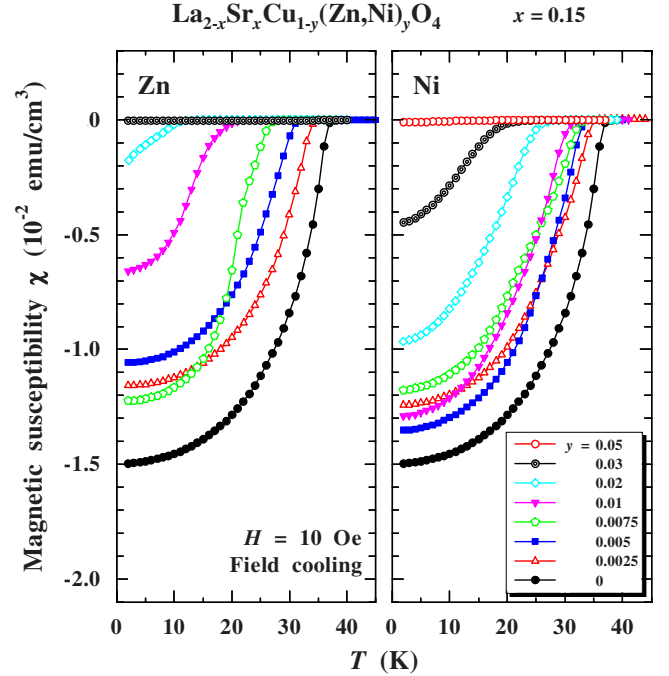


FIG. 5. (Color online) Temperature dependence of the magnetic susceptibility χ for $\text{La}_{2-x}\text{Sr}_x\text{Cu}_{1-y}(\text{Zn}, \text{Ni})_y\text{O}_4$ with $x=0.15$ and $y \leq 0.05$ in a magnetic field of 10 Oe on field cooling.

≤ 0.05 . T_c decreases with increasing y in both Zn- and Ni-substituted samples and disappears at $y(\text{Zn})=0.03$ and $y(\text{Ni})=0.05$, respectively. Moreover, it is found that the absolute value of χ at 2 K, $|\chi_{2\text{K}}|$, corresponding to the SC volume fraction decreases markedly with increasing y in both Zn- and Ni-substituted samples, and the decrease is more marked in the former than in the latter. These results suggest that the SC volume fraction decreases more markedly through the Zn substitution than through the Ni substitution, which is analogous to the results in $x=0.13$.¹²

3. Volume fractions of SC and magnetic regions

We estimated volume fractions of different states of Cu spins in one sample related to the three terms in Eq. (3.1) and two terms in Eq. (3.2) using the best-fit values of A_0 , A_1 , A_2 , and A_σ . Details of the estimation of the volume fractions were described in our previous paper.¹¹ It is noted in the estimation that the region expressed by A_1 , corresponding to the region in which the Cu spin fluctuations slow down and/or a short-range magnetic order is formed at low temperatures, is called the A_1 region. Similarly, regions expressed by A_0 , A_2 , and A_σ are called A_0 , A_2 , and A_σ regions, respectively. Volume fractions of A_0 , A_1 , A_2 , and A_σ regions are denoted as V_{A_0} , V_{A_1} , V_{A_2} , and V_{A_σ} , respectively. Figure 6 displays the impurity-concentration dependence of V_{A_0} , V_{A_1} , V_{A_2} , and V_{A_σ} at 0.3 K for $\text{La}_{2-x}\text{Sr}_x\text{Cu}_{1-y}(\text{Zn}, \text{Ni})_y\text{O}_4$ with $x=0.15$. For the Zn substitution, V_{A_0} rapidly decreases with increasing $y(\text{Zn})$ and becomes almost zero at $y(\text{Zn})=0.03$. Instead, V_{A_1} increases and becomes almost 100% at $y(\text{Zn})=0.03$, indicating that the Cu spin fluctuations slow down and/or the short-range magnetic order is formed in the whole

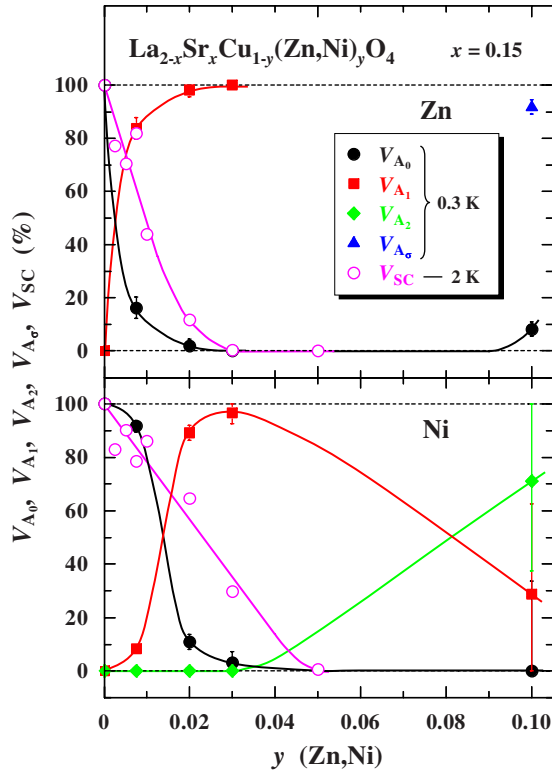


FIG. 6. (Color online) Impurity-concentration dependence of V_{A_0} (closed circles), V_{A_1} (closed squares), V_{A_2} (closed diamonds), and V_{A_σ} (closed triangles) estimated from the μ SR time spectra at 0.3 K in $\text{La}_{2-x}\text{Sr}_x\text{Cu}_{1-y}(\text{Zn,Ni})_y\text{O}_4$ with $x=0.15$. Impurity-concentration dependence of V_{SC} (open circles) estimated from the magnetic susceptibility at 2 K on field cooling is also plotted. V_{A_0} : Volume fraction of the region where Cu spins fluctuate fast beyond the μ SR frequency window. V_{A_1} : Volume fraction of the region where the Cu spin fluctuations slow down and/or a short-range magnetic order is formed. V_{A_2} : Volume fraction of the region where a long-range magnetic order is formed. V_{A_σ} : Volume fraction of the region with slightly larger magnetic moments of nuclear dipoles being randomly distributed. V_{SC} : Volume fraction of the superconducting region. Solid lines are to guide the reader's eye.

area of the sample of $y(\text{Zn})=0.03$. For $y(\text{Zn})=0.10$, V_{A_0} is not zero but about 10% and almost all area of the sample is covered with the A_σ region.

For the Ni substitution, on the other hand, the decrease in V_{A_0} is weak at $y(\text{Ni})=0.0075$, while V_{A_0} rapidly decreases for $y(\text{Ni})>0.0075$ and reaches zero at $y(\text{Ni})=0.05$. The trend that the formation of the magnetic order requires a larger amount of Ni than of Zn is the same as in the case of $x=0.13$.¹² The A_2 region starts to appear at $y(\text{Ni})=0.03-0.10$. In spite of large error bars of V_{A_0} , V_{A_1} , and V_{A_2} the temperature dependence of V_{A_2} allows us to conclude that the A_2 region is formed almost entirely in the sample of $y(\text{Ni})=0.10$.

Next, the SC volume fraction at 2 K, V_{SC} , was estimated from $|\chi_{2K}|$ shown in Fig. 5. The value of V_{SC} for each y is normalized by its value at $y=0$. The impurity-concentration dependence of V_{SC} is plotted in Fig. 6. For the Zn substitution, V_{SC} rapidly decreases with increasing $y(\text{Zn})$, changes to slowly decrease for $y(\text{Zn})\geq 0.02$, and finally disappears for

$y(\text{Zn})\geq 0.03$. The y dependence of V_{SC} for the Ni substitution is analogous to the y dependence of V_{SC} for the Zn substitution, although values of V_{SC} for $y(\text{Ni})=0.0025-0.01$ are scattered around 85%. The decrease is, however, weaker through the Ni substitution than through the Zn substitution. In comparison between the SC and magnetic volume fractions, the y dependence of V_{SC} and V_{A_0} is roughly similar to each other in qualitative viewpoint for the Zn substitution. For the Ni substitution, on the other hand, the tendency of the decrease in V_{SC} and V_{A_0} seems to be similar to each other. Therefore, at the lowest temperature of 0.3 K, the A_0 region is in rough correspondence to the SC region in both Zn- and Ni-substituted samples. These results are similar to those obtained in $x=0.13$,¹² in which the A_0 region is in rough correspondence to the SC region in both Zn- and Ni-substituted samples.

B. Effect of Zn substitution in $x=0.18$ and 0.20

The ZF- μ SR time spectra in $\text{La}_{2-x}\text{Sr}_x\text{Cu}_{1-y}\text{Zn}_y\text{O}_4$ with $x=0.18$ and 0.20 are shown in Fig. 1.^{25,26} Focusing on the spectra at low temperatures, fast depolarization of muon spins is observed at $y(\text{Zn})=0.02-0.03$ for $x=0.18$ and 0.20, although the depolarization is weaker than that of $x=0.15$ with $y(\text{Zn})=0.02-0.03$. Such behaviors can also be confirmed by the temperature dependence of A_0 that T_N^{onset} decreases with increasing x up to $x=0.20$.²⁶ This indicates that the Cu spin fluctuations slow down at low temperatures even in the overdoped regime of $\text{La}_{2-x}\text{Sr}_x\text{Cu}_{1-y}\text{Zn}_y\text{O}_4$, which is in sharp contrast with the conclusion by Panagopoulos *et al.*^{27,28} that the Zn-induced slowing down disappears above the possible quantum critical point of $x\sim 0.19$. The reason for the sharp contrast is that they made μ SR measurements not for $y(\text{Zn})=0.03$ but for $y(\text{Zn})=0.01, 0.02$ and 0.05.

Figure 7 shows the temperature dependence of χ on field cooling for $\text{La}_{2-x}\text{Sr}_x\text{Cu}_{1-y}\text{Zn}_y\text{O}_4$ with $x=0.18$ and 0.20 and $y\leq 0.03$. T_c decreases with increasing y and seems to disappear just above $y=0.03$ for both $x=0.18$ and 0.20. $|\chi_{2K}|$, on the other hand, is found to decrease progressively with increasing y for $y>0.0025$ and seems to be zero just above $y=0.03$ in both $x=0.18$ and 0.20. It is found in the y dependence of V_{SC} in Fig. 8 that V_{SC} 's of $x=0.18$ and 0.20 are roughly located on the same line. That is, the magnitude of the suppression of the SC volume fraction by the Zn substitution is similar to each other in the overdoped samples of $x=0.18$ and 0.20.

The Zn-concentration dependence of V_{A_0} at 0.3 K for $x=0.15, 0.18$, and 0.20 is shown in Fig. 8. V_{A_0} for $x=0.18$ and 0.20 was estimated from fitting the spectra using Eq. (3.1). With increasing x , the magnitude of the decrease in V_{A_0} with increasing y becomes small. As for the comparison between V_{SC} and V_{A_0} , V_{SC} is smaller than V_{A_0} for $x=0.18$ and 0.20 and vice versa for $x=0.15$, although decreases in V_{SC} and V_{A_0} with increasing y seem to be qualitatively similar to each other for $x=0.20$ as well as for $x=0.15$.

IV. DISCUSSION

A. Spatial distribution of SC and magnetic regions in the CuO_2 plane in the ground state

First, we discuss Zn- and Ni-concentration dependence of the SC and magnetic volume fractions at 0.3 K in the ground

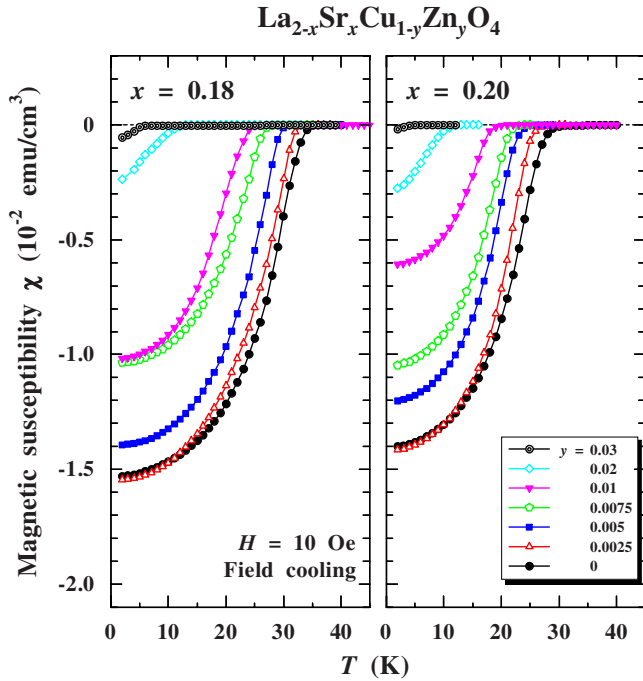


FIG. 7. (Color online) Temperature dependence of the magnetic susceptibility χ for $\text{La}_{2-x}\text{Sr}_x\text{Cu}_{1-y}\text{Zn}_y\text{O}_4$ with $x=0.18$ and 0.20 and $y \leq 0.03$ in a magnetic field of 10 Oe on field cooling.

state for $\text{La}_{2-x}\text{Sr}_x\text{Cu}_{1-y}(\text{Zn},\text{Ni})_y\text{O}_4$ with $x=0.15$. Figure 9 displays schematic pictures of the spatial distribution of A_0 and A_1 regions with different Cu spin states at 0.3 K for typical y values in $\text{La}_{2-x}\text{Sr}_x\text{Cu}_{1-y}(\text{Zn},\text{Ni})_y\text{O}_4$ with $x=0.15$, on the assumption that the magnetic order is developed around each Zn or Ni for lightly Zn- or Ni-substituted

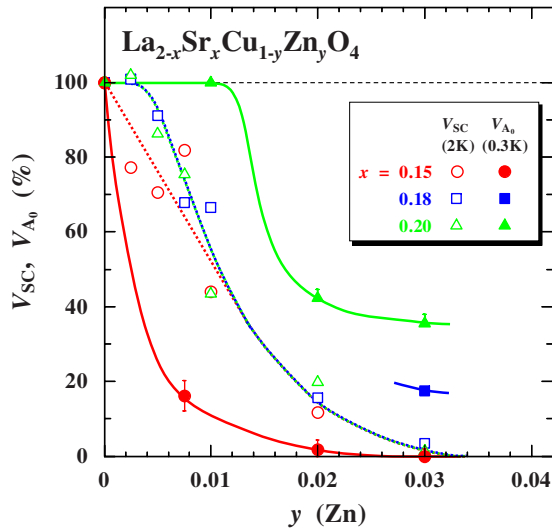


FIG. 8. (Color online) Zn-concentration dependence of V_{A_0} (closed symbols) estimated from the μSR time spectra at 0.3 K in $\text{La}_{2-x}\text{Sr}_x\text{Cu}_{1-y}\text{Zn}_y\text{O}_4$ with $x=0.15$, 0.18, and 0.20. Zn-concentration dependence of V_{SC} (open symbols) estimated from the magnetic susceptibility at 2 K on field cooling is also plotted. V_{A_0} : Volume fraction of the region where Cu spins fluctuate fast beyond the μSR frequency window. V_{SC} : Volume fraction of the superconducting region. Solid and dotted lines are to guide the reader's eye.

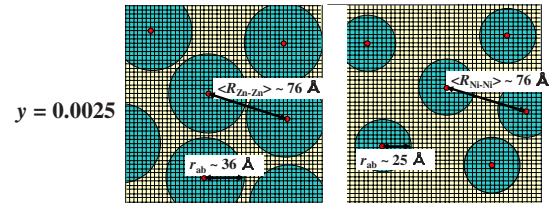
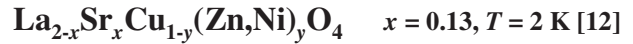
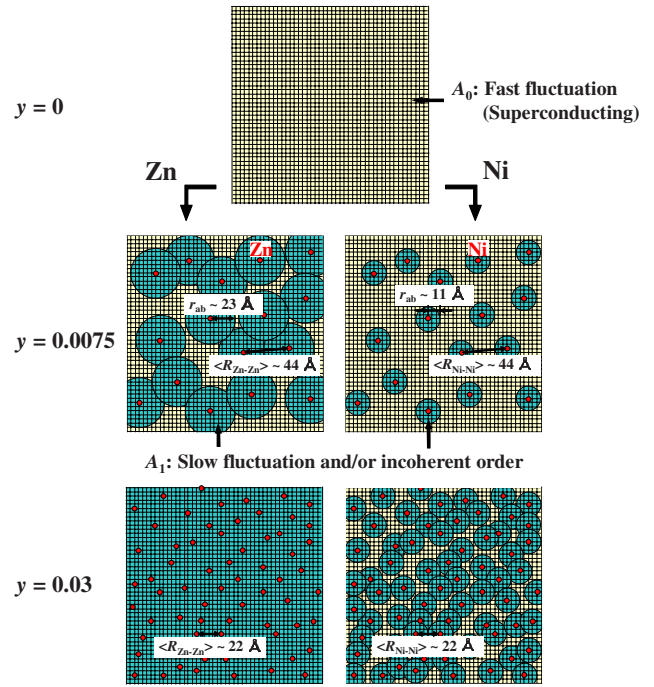


FIG. 9. (Color online) Schematic pictures of the spatial distribution of different Cu spin states in the CuO_2 plane, corresponding to A_0 and A_1 at 0.3 K for typical y values in $\text{La}_{2-x}\text{Sr}_x\text{Cu}_{1-y}(\text{Zn},\text{Ni})_y\text{O}_4$ with $x=0.15$. Each crossing point of the grid pattern represents the Cu site. Zn and Ni atoms are randomly distributed in the CuO_2 plane. Sizes of the circles are calculated from the ratio $V_{A_0} : V_{A_1}$ in each y . r_{ab} indicates the radius of the A_1 region around each Zn or Ni. $\langle R_{\text{Zn-Zn}} \rangle$ and $\langle R_{\text{Ni-Ni}} \rangle$ indicate mean distances between Zn atoms and between Ni atoms, respectively. Similar schematic pictures of $x=0.13$ are also shown for comparison (Ref. 12).

samples. This assumption has not yet been confirmed directly but it is reasonable referring to the results of scanning-tunneling-microscopy measurements in the Zn- or Ni-substituted $\text{Bi}_2\text{Sr}_2\text{CaCu}_{2-y}(\text{Zn},\text{Ni})_y\text{O}_{8+\delta}$.^{29,30} Sizes of the circles were calculated from the ratio $V_{A_0} : V_{A_1}$ in each y . It is noted from the calculation in each y that the size of the circle was found to be almost independent of y . For the impurity-free sample of $y=0$, the A_0 region covers the whole area of the CuO_2 plane where the superconductivity appears. Through the 0.75% substitution of Zn for Cu, A_1 regions, namely, slowly fluctuating and/or short-range magnetically ordered regions of Cu spins are formed with the radius $r_{ab} \sim 23 \text{ \AA}$ around each Zn in the A_0 region, namely, in the fast

fluctuating sea of Cu spins. It is found that a large part of the CuO_2 plane is covered with A_1 regions, so that V_{SC} in rough correspondence to V_{A_0} is strongly diminished. In comparison between r_{ab} and the mean distance between Zn atoms $\langle R_{\text{Zn-Zn}} \rangle \sim 44 \text{ \AA}$ at $y(\text{Zn})=0.0075$, A_1 regions overlap one another mostly. With increasing $y(\text{Zn})$, A_1 regions become dominant and the whole area of the CuO_2 plane is covered with A_1 regions for $y(\text{Zn})=0.03$, indicating that the superconductivity is completely suppressed. In the case of $x=0.13$, once A_1 regions start to overlap one another, A_2 regions corresponding to a long-range magnetically ordered regions start to develop.¹¹ For $x=0.15$, on the contrary, A_2 regions are not generated in spite of the overlap between A_1 regions. The reason may be due to a shorter-range magnetic order in $x=0.15$ than in $x=0.13$.

For the Ni substitution, on the other hand, A_1 regions appear through the 0.75% substitution and r_{ab} is estimated to be $\sim 11 \text{ \AA}$, which is smaller than that around Zn. This indicates that A_1 regions do not overlap one another mostly. For $y(\text{Ni})=0.03$, a large part of the CuO_2 plane is covered with A_1 regions. These changes with increasing y for both Zn- and Ni-substituted samples suggest that the SC region competes with slowly fluctuating and/or short-range magnetically ordered regions of Cu spins.

As seen in the case of $y=0.0075$, the size of each A_1 region is larger around Zn than around Ni, which is similar to the case of $x=0.13$ shown in Fig. 9.¹² Itoh *et al.*³¹ have reported from NQR measurements in the Zn- and Ni-substituted $\text{YBa}_2(\text{Cu}_{1-y}\text{M}_y)_4\text{O}_8$ ($M=\text{Zn}, \text{Ni}$) that the size of the wipeout region where the Cu spin correlation is developed is $\sim 6 \text{ \AA}$ around Zn; while in the case of Ni, it is limited just on the Ni site. The difference between Zn and Ni substitution is qualitatively similar to that in our present results. The quantitative difference between the NQR and our μSR results is probably due to the difference that the time scale of the Cu spin fluctuations observed by NQR is longer than that by μSR . It is noted, on the other hand, that Ouazi *et al.*³² have reported contrasting results on the Zn- and Ni-substitution effects from NMR measurements in partially Zn- and Ni-substituted $\text{YBa}_2\text{Cu}_3\text{O}_7$. They have suggested that both Zn and Ni induce a staggered paramagnetic polarization with the typical extension $\xi=3$ cell units for Zn and $\xi \geq 3$ for Ni, which is inconsistent with our model and Ref. 31, although the exact reason has not yet been clarified.

As for the difference between results in $x=0.15$ and in $x=0.13$, as shown in the case of $x=0.15$ and $y=0.0075$ and the case of $x=0.13$ and $y=0.0025$ in Fig. 9, r_{ab} is smaller in $x=0.15$ even at 0.3 K than in $x=0.13$ at 2 K for both Zn and Ni substitution. This indicates that the development of the Cu spin correlation around Zn and Ni is less in $x=0.15$ than in $x=0.13$. The reason is discussed in Sec. IV C.

B. Effect of Ni substitution

Nakano *et al.*³³ have insisted from χ measurements in $\text{La}_{2-x}\text{Sr}_x\text{Cu}_{1-y}\text{Ni}_y\text{O}_4$ that Ni tends to be substituted as Ni^{3+} (the spin quantum number $S=1/2$) instead of Ni^{2+} for $y(\text{Ni}) \leq 0.01$ in $x=0.15$. Moreover, Matsuda *et al.*³⁴ and Hiraka *et al.*³⁵ have insisted from neutron-scattering experi-

ments in $\text{La}_{2-x}\text{Sr}_x\text{Cu}_{1-y}\text{Ni}_y\text{O}_4$ with $x=0.05-0.07$ that Ni tends to be substituted as Ni^{3+} or the substituted Ni^{2+} tends to trap a hole and form the so-called Zhang-Rice singlet state at low temperatures in which the hole is localized, leading to the decrease in the effective hole concentration p_{eff} as in the case of doped La_2NiO_4 .^{36,37} In any case, Ni spins are effectively regarded as $S=1/2$, suggesting that the Ni substitution for Cu does not destroy the Cu spin correlation with $S=1/2$. In the present results, however, the depolarization of muon spins in the μSR time spectra becomes fast progressively with increasing $y(\text{Ni})$ as shown in Figs. 1 and 2, indicating the development of the Cu spin correlation.

On the other hand, one may claim that the decrease in p_{eff} by the Ni substitution results in transfer into the underdoped regime, leading to the development of the Cu spin correlation. Supposed that each Ni traps a hole, for example, p_{eff} of the 2% Ni-substituted sample with $x=0.15$ should be in correspondence to that of the Ni-free sample with $x=0.13$. This is, however, inconsistent with the result that the former shows a fast depolarization of muon spins as shown in Fig. 1 while the latter does not at 2 K.¹² Therefore, it appears that Ni does not necessarily trap one hole exactly for the optimally doped $x=0.15$ in comparison with $x=0.05-0.07$.^{34,35} In any case, further experiments are necessary to draw a conclusion.

C. Relation to the spin-charge stripe order

As mentioned in Sec. I, in the case of $x=0.13$, it has been concluded that non-SC regions around Zn and Ni are in correspondence to regions where the dynamical stripe correlations of spins and holes are pinned and localized to be a static stripe order by Zn and Ni.¹² For the Zn substitution, r_{ab} estimated at 2 K shows the maximum around $x=0.115$ in $x=0.10-0.13$.¹¹ As mentioned above, moreover, r_{ab} is smaller in $x=0.15$ even at 0.3 K than in $x=0.13$ at 2 K. This is also the case for the Ni substitution. This nonmonotonic x dependence of r_{ab} eliminates the explanation that the magnetically ordered regions around impurities become small due to weakening of the Cu spin correlation by doped holes. Rather, this result suggests that the dynamical stripe correlations are pinned and localized around Zn and Ni, leading to the formation of the static stripe order. This is because the dynamical stripe correlations develop most around $x=0.115$.³⁸ In fact, from elastic neutron-scattering measurements in $\text{La}_{2-x}\text{Sr}_x\text{Cu}_{1-y}(\text{Zn}, \text{Ni})_y\text{O}_4$ with $x=0.15$,⁶ incommensurate elastic magnetic peaks corresponding to the formation of the static spin stripe order have been confirmed for $y(\text{Zn})=0.017$ and for $y(\text{Ni})=0.029$.

To summarize, the present results can be understood by the concept of the stripe pinning that the dynamical stripe correlations are pinned and localized around Zn and Ni, so that the static stripe order is formed and frequencies of the Cu spin fluctuations come into the μSR frequency window at low temperatures. The difference in size of the non-SC and stripe-pinned region between Zn- and Ni-substituted samples can be interpreted as described precisely in the former paper,¹² taking into account the difference in the total energy of the superexchange energy between Cu spins and

the transfer integral of holes between two cases: one is the case where Zn or Ni is located at a charge (hole) stripe and the other is the case where Zn or Ni is at a spin stripe.

D. Comparison with neutron-scattering results

Kimura *et al.*⁵ and Kofu *et al.*⁶ have reported from inelastic neutron-scattering experiments in $\text{La}_{2-x}\text{Sr}_x\text{Cu}_{1-y}(\text{Zn},\text{Ni})_y\text{O}_4$ with $x=0.15$ that a gap opens in the low-energy spin excitation spectrum for the impurity-free sample of $y=0$, while an in-gap state appears through the Zn substitution so that incommensurate elastic magnetic peaks are observed for $y(\text{Zn}) \geq 0.017$. For the Ni substitution, on the other hand, the gap energy decreases with increasing $y(\text{Ni})$ and incommensurate elastic magnetic peaks are observed for $y(\text{Ni}) \geq 0.029$. Our present results that the formation of the magnetic order requires a larger amount of Zn than of Ni are consistent with their neutron-scattering results that elastic magnetic peaks start to be observed at $y(\text{Zn})=0.017$ and $y(\text{Ni})=0.029$. On the other hand, slowing down of the Cu spin fluctuations is observed below 2 K in the μSR time spectra for $y(\text{Zn})=0.0075$, while incommensurate elastic magnetic peaks are unobservable down to 1.5 K in the neutron-scattering measurements for $y(\text{Zn}) \sim 0.0075$. These suggest that the Cu spin correlation is locally developed only around Zn or Ni and is detectable by means of μSR being able to probe the local Cu spin correlation. This is consistent with our proposed model shown in Fig. 9.

E. Relation between the Cu spin dynamics and superconductivity in the overdoped regime

For the Zn-substituted samples of $x \leq 0.15$, V_{A_0} and V_{SC} are in rough correspondence to each other, suggesting that the non-SC region around Zn roughly corresponds to the region where the dynamical stripe correlations are pinned and stabilized.¹¹ In the overdoped regime of $x=0.20$, as shown in Fig. 8, the y dependence of V_{A_0} and V_{SC} seems to be similar to each other from the qualitative viewpoint. This suggests that the superconductivity is realized in a region in which Cu spins fluctuate fast beyond the μSR frequency window even in the overdoped regime. It is noted for $x=0.20$ that V_{A_0} starts to decrease with increasing $y(\text{Zn})$ above $y(\text{Zn})=0.01$, suggesting that more than 1% Zn is required for the pinning and stabilization of the dynamical stripe correlations due to weakening of the Cu spin correlation in the overdoped regime.

It is found that V_{SC} is larger than V_{A_0} in each y for $x=0.15$. In the overdoped regime of $x=0.20$, on the other hand, V_{SC} is smaller than V_{A_0} in each y . One may claim that in the overdoped regime, the development of the Cu spin correlation tends to be weakened and temperatures lower than 0.3 K are needed to observe the development of the Cu spin correlation. We have performed, however, ZF- μSR measurements for $x=0.20$ and $y(\text{Zn})=0.03$ down to 0.02 K and found almost no development of the Cu spin correlation more than at 0.3 K.^{25,26} The smaller V_{SC} than V_{A_0} in the overdoped regime of $x=0.20$ is possibly explained by the inhomogeneity of superconductivity. Formerly, transverse-

field μSR experiments have revealed the decrease in the SC carrier density with increasing hole concentration in the overdoped regime of $\text{Tl}_2\text{Ba}_2\text{CuO}_{6+\delta}$.³⁹⁻⁴¹ Moreover, χ measurements have revealed the decrease in the SC volume fraction with increasing hole concentration in the overdoped regime of $\text{La}_{2-x}\text{Sr}_x\text{CuO}_4$.⁴²⁻⁴⁶ This suggests the occurrence of a phase separation into SC and normal-state regions in the overdoped high- T_c cuprates. For $x=0.20$, it is considered that a small amount of non-SC regions is formed in the CuO_2 plane. In this case, due to the reduction in the SC volume fraction in the phase-separated state, it is reasonable that V_{SC} is smaller than V_{A_0} in each y for $x=0.20$.

To summarize, it appears that, in the overdoped regime where the phase separation into SC and normal-state regions takes place, the dynamical stripe correlations are pinned and localized around Zn in the SC region, resulting in the decrease in V_{A_0} and V_{SC} . With increasing x , owing to the decrease in the SC volume fraction and weakening of the Cu spin correlation, it is possible that the volume fraction of the slowly fluctuating and/or short-range magnetically ordered region of Cu spins decreases and finally reaches zero at the boundary between the SC and normal-state phases in $\text{La}_{2-x}\text{Sr}_x\text{CuO}_4$.^{25,26,47}

V. SUMMARY

Effects of Zn and Ni impurities on the Cu spin dynamics and superconductivity have been investigated from the ZF- μSR and χ measurements for the optimally doped and overdoped $\text{La}_{2-x}\text{Sr}_x\text{Cu}_{1-y}(\text{Zn},\text{Ni})_y\text{O}_4$ with $x=0.15, 0.18$ and 0.20 , changing y up to 0.10 in fine step. In the optimally doped $x=0.15$, the ZF- μSR measurements have revealed that, for both Zn- and Ni-substituted samples, the Cu spin fluctuations start to exhibit slowing down at $y=0.0075$ with increasing y . The depolarization of muon spins is, however, faster in the Zn-substituted sample than in the Ni-substituted one. These results indicate that the formation of a magnetic order requires a larger amount of Ni than of Zn, which is similar to our previous results for $x=0.13$. The χ measurements have revealed that the SC volume fraction strongly decreases by a small amount of Zn and the decrease is more marked than by a small amount of Ni, which is also similar to our previous results for $x=0.13$.

From the estimation of volume fractions of the SC and magnetic regions for $x=0.15$, it has been found that the size of each region where Cu spin fluctuations exhibit slowing down is larger around Zn than around Ni, which is similar to the case of $x=0.13$. Moreover, it has been found that the region where Cu spins fluctuate fast beyond the μSR frequency window is in rough correspondence to the SC region in both Zn- and Ni-substituted samples. According to the concept of the stripe pinning, it follows that the dynamical stripe correlations of spins and holes are pinned and localized around Zn and Ni even for $x=0.15$, leading to the formation of the static stripe order and the suppression of superconductivity. This may indicate an importance of the dynamical stripe in the appearance of the high- T_c superconductivity in the hole-doped cuprates.

As for the overdoped regime of $x=0.18$ and 0.20 , Zn-induced slowing down of the Cu spin fluctuations has also been observed for $y(\text{Zn})=0.02-0.03$, although the slowing down has been weakened progressively with an increase in x . This suggests the occurrence of the stripe pinning even in the overdoped regime. In comparison between volume fractions of SC and magnetic regions, the region where Cu spins fluctuate fast beyond the μSR frequency window seems to be in rough correspondence to the SC region even in the overdoped regime. It appears that a pinning and stabilization of the dynamical stripe correlations take place in the SC regions

in the phase-separated state composed of SC and normal-state regions in the overdoped high- T_c cuprates.

ACKNOWLEDGMENTS

This work was partly supported by Joint Programs of the Japan Society for the Promotion of Science; by a TORAY Science and Technology Grant; and also by a Grant-in-Aid for Scientific Research from the Ministry of Education, Culture, Sports, Science and Technology, Japan.

*Corresponding author; adachi@teion.apph.tohoku.ac.jp

[†]Present address: Department of Physics, Faculty of Mathematics and Natural Sciences, Padjadjaran University, Jl. Raya Bandung-Sumedang Km. 21 Jatinangor, West Jawa, Indonesia 45363.

- ¹G. Xiao, M. Z. Cieplak, J. Q. Xiao, and C. L. Chien, *Phys. Rev. B* **42**, 8752 (1990).
- ²For example, see M. Tinkham, *Introduction to Superconductivity* (McGraw-Hill, New York, 1975).
- ³Y. Kitaoka, K. Ishida, and K. Asayama, *J. Phys. Soc. Jpn.* **63**, 2052 (1994).
- ⁴Y. Sidis, P. Bourges, H. F. Fong, B. Keimer, L. P. Regnault, J. Bossy, A. Ivanov, B. Hennion, P. Gautier-Picard, G. Collin, D. L. Millius, and I. A. Aksay, *Phys. Rev. Lett.* **84**, 5900 (2000).
- ⁵H. Kimura, M. Kofu, Y. Matsumoto, and K. Hirota, *Phys. Rev. Lett.* **91**, 067002 (2003).
- ⁶M. Kofu, H. Kimura, and K. Hirota, *Phys. Rev. B* **72**, 064502 (2005).
- ⁷I. Watanabe, T. Adachi, K. Takahashi, S. Yairi, Y. Koike, and K. Nagamine, *Phys. Rev. B* **65**, 180516(R) (2002).
- ⁸I. Watanabe, T. Adachi, K. Takahashi, S. Yairi, Y. Koike, and K. Nagamine, *J. Phys. Chem. Solids* **63**, 1093 (2002).
- ⁹I. Watanabe, T. Adachi, S. Yairi, Y. Koike, and K. Nagamine, *Physica B (Amsterdam)* **326**, 305 (2003).
- ¹⁰T. Adachi, I. Watanabe, S. Yairi, K. Takahashi, Y. Koike, and K. Nagamine, *J. Low Temp. Phys.* **131**, 843 (2003).
- ¹¹T. Adachi, S. Yairi, K. Takahashi, Y. Koike, I. Watanabe, and K. Nagamine, *Phys. Rev. B* **69**, 184507 (2004).
- ¹²T. Adachi, S. Yairi, Y. Koike, I. Watanabe, and K. Nagamine, *Phys. Rev. B* **70**, 060504(R) (2004).
- ¹³J. M. Tranquada, B. J. Sternlieb, J. D. Axe, Y. Nakamura, and S. Uchida, *Nature (London)* **375**, 561 (1995).
- ¹⁴S. A. Kivelson, E. Fradkin, and V. J. Emery, *Nature (London)* **393**, 550 (1998).
- ¹⁵Y. Koike, S. Takeuchi, H. Sato, Y. Hama, M. Kato, Y. Ono, and S. Katano, *J. Low Temp. Phys.* **105**, 317 (1996).
- ¹⁶Y. Koike, S. Takeuchi, Y. Hama, H. Sato, T. Adachi, and M. Kato, *Physica C* **282-287**, 1233 (1997).
- ¹⁷T. Adachi, T. Noji, H. Sato, Y. Koike, T. Nishizaki, and N. Kobayashi, *J. Low Temp. Phys.* **117**, 1151 (1999).
- ¹⁸Y. Koike, T. Adachi, N. Oki, Risdiana, M. Yamazaki, T. Kawamata, T. Noji, K. Kudo, N. Kobayashi, I. Watanabe, and K. Nagamine, *Physica C* **426**, 189 (2005).
- ¹⁹T. Adachi, N. Oki, Risdiana, S. Yairi, Y. Koike, and I. Watanabe, *Physica C* **460-462**, 1172 (2007).
- ²⁰Y. J. Uemura, T. Yamazaki, D. R. Harshman, M. Senba, and E. J. Ansaldo, *Phys. Rev. B* **31**, 546 (1985).
- ²¹On the analogy of the results for $y(\text{Zn})=0.10$ in $x=0.13$ (Ref. 11) a magnetic order is destroyed by a large amount of nonmagnetic Zn at $y(\text{Zn})=0.10$ in $x=0.15$. In this case, Cu spins no longer produce large magnetic moments corresponding to an exponential-like fast depolarization of muon spins but might produce slightly larger magnetic moments than nuclear moments, leading to Gaussian-type depolarization with a rather narrow width.
- ²²E. Torikai, I. Tanaka, H. Kojima, H. Kitazawa, and K. Nagamine, *Hyperfine Interact.* **63**, 271 (1990).
- ²³I. Watanabe, K. Kawano, K. Kumagai, K. Nishiyama, and K. Nagamine, *J. Phys. Soc. Jpn.* **61**, 3058 (1992).
- ²⁴I. Watanabe, K. Nishiyama, K. Nagamine, K. Kawano, and K. Kumagai, *Hyperfine Interact.* **86**, 603 (1994).
- ²⁵Risdiana, T. Adachi, N. Oki, S. Yairi, Y. Tanabe, K. Omori, T. Suzuki, I. Watanabe, A. Koda, W. Higemoto, and Y. Koike, *Physica C* **460-462**, 874 (2007).
- ²⁶Risdiana, T. Adachi, N. Oki, S. Yairi, Y. Tanabe, K. Omori, Y. Koike, T. Suzuki, I. Watanabe, A. Koda, and W. Higemoto, *Phys. Rev. B* **77**, 054516 (2008).
- ²⁷C. Panagopoulos, J. L. Tallon, B. D. Rainford, T. Xiang, J. R. Cooper, and C. A. Scott, *Phys. Rev. B* **66**, 064501 (2002).
- ²⁸C. Panagopoulos, A. P. Petrovic, A. D. Hillier, J. L. Tallon, C. A. Scott, and B. D. Rainford, *Phys. Rev. B* **69**, 144510 (2004).
- ²⁹S. H. Pan, E. W. Hudson, K. M. Lang, H. Eisaki, S. Uchida, and J. C. Davis, *Nature (London)* **403**, 746 (2000).
- ³⁰E. W. Hudson, K. M. Lang, V. Madhavan, S. H. Pan, H. Eisaki, S. Uchida, and J. C. Davis, *Nature (London)* **411**, 920 (2001).
- ³¹Y. Itoh, T. Machi, N. Watanabe, and N. Koshizuka, *J. Phys. Soc. Jpn.* **70**, 644 (2001).
- ³²S. Ouazi, J. Bobroff, H. Alloul, M. Le Tacon, N. Blanchard, G. Collin, M. H. Julien, M. Horvatić, and C. Berthier, *Phys. Rev. Lett.* **96**, 127005 (2006).
- ³³T. Nakano, N. Momono, T. Nagata, M. Oda, and M. Ido, *Phys. Rev. B* **58**, 5831 (1998).
- ³⁴M. Matsuda, M. Fujita, and K. Yamada, *Phys. Rev. B* **73**, 140503(R) (2006).
- ³⁵H. Hiraka, S. Ohta, S. Wakimoto, M. Matsuda, and K. Yamada, *J. Phys. Soc. Jpn.* **76**, 074703 (2007).
- ³⁶J. Zaanen and A. M. Oleś, *Phys. Rev. B* **48**, 7197 (1993).
- ³⁷E. Pellegrin, J. Zaanen, H.-J. Lin, G. Meigs, C. T. Chen, G. H. Ho, H. Eisaki, and S. Uchida, *Phys. Rev. B* **53**, 10667 (1996).

- ³⁸K. Yamada, C. H. Lee, K. Kurahashi, J. Wada, S. Wakimoto, S. Ueki, H. Kimura, Y. Endoh, S. Hosoya, G. Shirane, R. J. Birgeneau, M. Greven, M. A. Kastner, and Y. J. Kim, *Phys. Rev. B* **57**, 6165 (1998).
- ³⁹Y. J. Uemura, A. Keren, L. P. Le, G. M. Luke, W. D. Wu, Y. Kubo, T. Manako, Y. Shimakawa, M. Subramanian, J. L. Cobb, and J. T. Markert, *Nature (London)* **364**, 605 (1993).
- ⁴⁰Ch. Niedermayer, C. Bernhard, U. Binninger, H. Glückler, J. L. Tallon, E. J. Ansaldo, and J. I. Budnick, *Phys. Rev. Lett.* **71**, 1764 (1993).
- ⁴¹Y. J. Uemura, *Solid State Commun.* **126**, 23 (2003).
- ⁴²Y. Tanabe, T. Adachi, T. Noji, and Y. Koike, *J. Phys. Soc. Jpn.* **74**, 2893 (2005).
- ⁴³Y. Tanabe, T. Adachi, T. Noji, H. Sato, and Y. Koike, *Low Temperature Physics: 24th International Conference on Low Temperature Physics - LT24*, AIP Conf. Proc. No. 850 (AIP, New York, 2006), p. 419.
- ⁴⁴T. Adachi, Y. Tanabe, T. Noji, H. Sato, and Y. Koike, *Physica C* **445-448**, 14 (2006).
- ⁴⁵Y. Tanabe, T. Adachi, K. Omori, H. Sato, and Y. Koike, *Physica C* **460-462**, 376 (2007).
- ⁴⁶Y. Tanabe, T. Adachi, K. Omori, H. Sato, T. Noji, and Y. Koike, *J. Phys. Soc. Jpn.* **76**, 113706 (2007).
- ⁴⁷S. Wakimoto, H. Zhang, K. Yamada, I. Swainson, H. Kim, and R. J. Birgeneau, *Phys. Rev. Lett.* **92**, 217004 (2004).